ISSN: 0067-2904

Evaluation of the Land Cover Changes in Mosul City, Iraq, Using Remote Sensing and GIS

Noor Z. Karam*, Bushra A. Ahmed
University of Baghdad/Collage of Sciences/ Department of Remote Sensing & GIS

Received: 5/7/2024 Accepted: 1/12/2024 Published: 30/1/2026

Abstract

Remote sensing techniques have been utilized to assess and manage natural resources in general and vegetation, in particular, to preserve the sustainability of plant wealth, evaluate and explain the current state of the vegetation condition, and determine the changes that occur to it as a result. Mosul's forests are exposed to many fires, including in 2017, 2021, and 2022. This study used Landsat8 satellite images and Geographic Information Systems (GIS). Some spectral indices were used, such as the Normalized Difference Vegetation Index (NDVI), Soil Adjusted Vegetation Index (SAVI), and Enhanced Vegetation Index 2 (EVI2). Land Surface Temperature (LST) was also calculated, in addition to the Normalized Difference Built-up Index (NDBI) and Normalized Difference Water Index (NDWI). LST was used to evaluate the extent to which plants are affected by the land surface temperature in Mosul city. According to the rate for the three years, the EVI2 index for the fourth month of 2023 had the highest vegetation, at 21.70%, while the NDVI index for the sixth month of 2015 had the lowest percentage. This study discovered that temperatures and fire clarity affect the vegetation cover rate, noting that the areas that have decreased and changed the most were those exposed to fires in 2017 and 2022.

Keywords: GIS, Mosul's forests, NDVI, SAVI, EVI2, and LST.

تقييم تغيرات الغطاء الأرضي في مدينة الموصل، العراق باستخدام تقنيات الاستشعار عن بعد ونظم المعلومات الجغرافية

نور كرم* ، بشرى علي احمد
قسم , كلية العلوم, جامعة بغداد, بغداد, العراق

الخلاصه:

استخدمت تطبيقات الاستشعار عن بعد لتقييم وإدارة الموارد الطبيعية بشكل عام والغطاء النباتي بشكل خاص للحفاظ على استدامة الثروة النباتية، وتقييم وتفسير الوضع الحالي لحالة الغطاء النباتي، وكذلك تقييم التغيرات التي تطرأ عليه. حيث تتعرض غابات الموصل بشكل خاص للعديد من الحرائق ومنها في الأعوام 2017 و2021 و2022، كما أنها تتأثر بارتفاع درجة حرارة سطح الأرض في الموصل بشكل عام. تم تقييم

*Email: Noor. karam2209m@sc.uobaghdad.edu.iq

نسبة الغطاء النباتي للأعوام 2015 و2020 و2023 لفصلي الربيع والصيف ومدى انتشارهما. باستخدام صور الأقمار الصناعية Landsat8 وبرامجيات المعلومات الجغرافية (GIS)، لوحظت المناطق المتضررة من أحداث الحرائق من خلال حساب المؤشرات الطيفية، ومؤشر الاختلاف الطبيعي للغطاء النباتي (NDVI)، ومؤشر الغطاء النباتي المعدل للتربة (SAVI)، ومؤشر الغطاء النباتي المحسن 2 (EVI2)، تم أيضًا حساب درجة حرارة سطح الأرض (LST)، ومؤشر الفرق المعياري المدمج (NDBI)، ومؤشر الماء المعياري للفرق (NDWI). استخدم مؤشر درجة الحرارة لتقييم مدى تأثر النباتات بدرجة حرارة سطح الأرض في مدينة الموصل. ارتباط بيرسون والانحدار الخطي البسيط بين مؤشرات الغطاء النباتي وLST استخدم لتحديد مدى تعرض الغطاء النباتي لدرجة الحرارة والحرائق. أما المعدل للسنوات الثلاث فقد تبين أن أعلى نسبة كانت لمؤشر EVI2 لعام 2023 الشهر الرابع وبلغت 21.70%، وأقل نسبة كانت لمؤشر NDVI لعام 2015 الشهر السادس. توصلت هذه الدراسة إلى تأثير درجات الحرارة ووضوح الحرائق على معدل الغطاء النباتي، مع ملاحظة أن المناطق التي انخفضت وتغيرت أكثر هي المناطق التي تعرضت للحرائق في عامي 2017 و2022.

1.Introduction

Vegetation cover represents an indicator and measure of environmental deterioration. Changes in the percentage of vegetation cover significantly impact land cover and general land use. Vegetation cover must be monitored continuously, and positive and negative changes must be studied [1]. Vegetation cover significantly impacts the terrestrial ecosystem, climate, and social and economic sectors. Land cover refers to the distribution and type of vegetation (such as trees and forests) that cover the surface of the Earth [2]. Changes in land cover resulting from natural and human sources are represented by biophysical changes that have noticeable effects on the quality of the ecosystem. Therefore, land cover changes can be a major indicator of environmental (ecological) changes on temporal and spatial scales, as discovering them and evaluating spatial and temporal changes is a major priority for researchers[3]. To study the changes in land cover, data must be collected that indicate the area's state at various times. Remote sensing by satellite in conjunction with GIS represents an effective and powerful tool in terms of speed, accuracy, and cost, as well as providing valuable information in many fields, as well as the ability of satellites to cover large areas that are difficult to achieve as they can be passed repeatedly, as well as the quality (spatial resolution) of the resulting image data. Sensor-based techniques have been applied [4]. Remote monitoring has been widely used in many studies that focused on detecting changes in land cover [5], [6], and [7]. Physical characteristics such as climate, soil quality, topography, groundwater, and surface water are reflected on the Earth's surface in vegetation or barren land. These factors determine whether the surface is thriving with vegetation or barren. This can be determined by analyzing satellite image data to identify indicators of vegetation cover and LST. The indicators show the condition of the Earth’s surface based on the degree of absorption and reflection in different regions of the spectrum of electromagnetic radiation (spectral bands). using specific spectral bands[8],[9],and [10]. LST plays a fundamental role in many environmental characteristics and has been used in many applications, including climatology, meteorology, and hydrology[11],[12]. It is important in agricultural management through remote sensing, as it represents an essential element in assessing water needs and timing of irrigation [13],[14]. Many studies have used remote sensing techniques and data to determine land cover change in various geographical situations. This study aims to assess changes in land cover inside Mosul, Iraq, using Landsat-8 satellite images and calculating the statistical parameters of NDVI and GNDVI indices. They concluded that there was a revealed geographical variance in vegetation cover from

2014 to 2018 [15]. (Rahman M. M,) he used the NDVI index to detect areas of vegetation, whereas he used Delta Cue to detect areas of vegetation change. He concluded that Using Landsat images from January 1989, January 2001, and January 2010 can determine the variation in vegetation coverage associated with afforestation and deforestation in the Patuakhali district [16], assessed land cover changes in the Fashiakhali Wildlife Sanctuary (FKWS) impact region over three decades (1994-2021). He used the NDVI, the Adjusted SAVI, and the link between LST and NDVI [17], compared the efficacy of several LST methods utilizing Landsat 8 day and night data and in situ observations. In addition to analyze LST approaches, the effects of six LSE models based on the NDVI were investigated[18].

2.Study area

Figure 1 depicts the location of the study area. Mosul city is located in the Boundary of the limits of Nineveh Governorate and covers an area of 180 km^2 [19]. The city's coordinates are Latitude of 36°21'25.9"N and longitude of 43°09'22.2"E. Mosul is located in northwestern Iraq on the western bank of the Tigris River, 400 kilometers north of Baghdad[15]. Mosul's temperature ranges from -3°C to 8°C in the winter and from 30°C to 46°C in the summer. Mosul's forests have seen several fires. Thus, it is vital to analyze the changes in the city and map vegetation cover and land surface temperature.

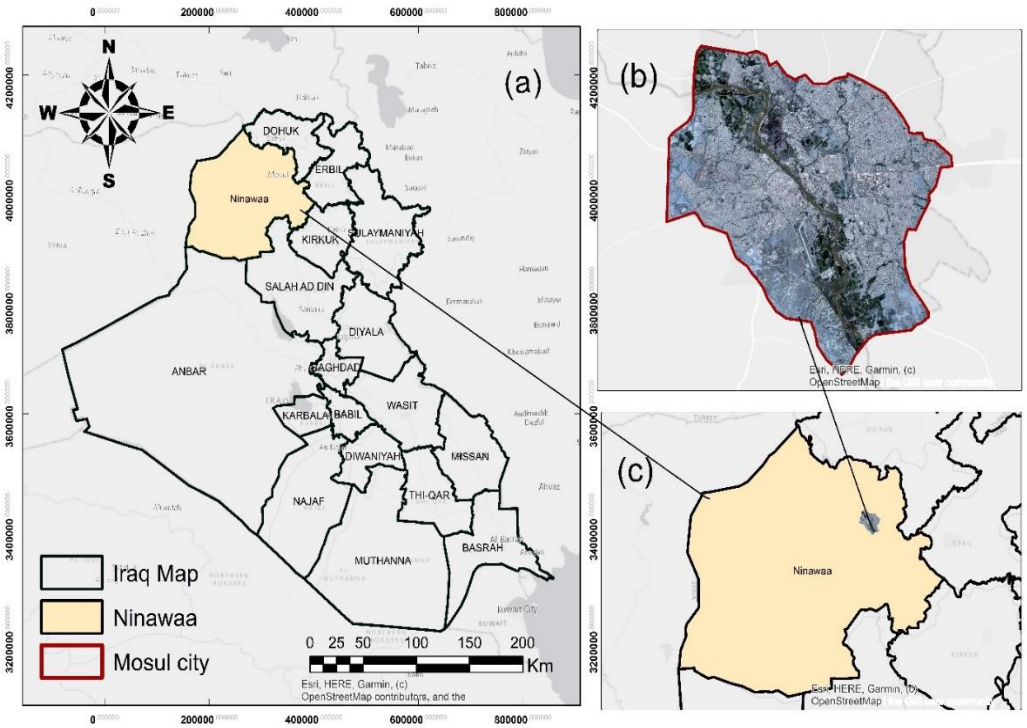

Figure 1: The study area map includes (a) Iraq, (b) Mosul City, and (c) Ninawa Governorate.

Contour maps are important maps that illustrate the nature of the terrain and the land's direction and degree of slope. They are imaginary lines that connect all points of equal height relative to sea level. Contour lines represent the height of mountains and calculate the degrees of slope. By working with the Arc Map program and the digital elevation file (DEM), several maps can be extracted that address the subject of the real shape of the study area, the most important of which are the appearance direction maps and the slope maps, to provide a

realistic, accurate and practical picture for extrapolating the digital spacing model to contribute to creating a spatial database related to the terrain of the study area, which can be significantly benefited from in scientific and applied fields [20]. It is clear from the visual analysis of Map (A) that the surface of the study area begins to rise as moving westward where, noticing that the highest point is 339 above sea level, with the presence of density and convergence of contour lines in the western part of the study area, which indicates the presence of a relative height, and on the contrary, it gradually decreases as moving east and southeast from the lowest point, which is 211 above sea level. ALOS PALSAR satellite images with a resolution of 12.5m were obtained from the website https://search.asf.alaska.edu/#. Figures (2) and (3) show the topography of the study area.

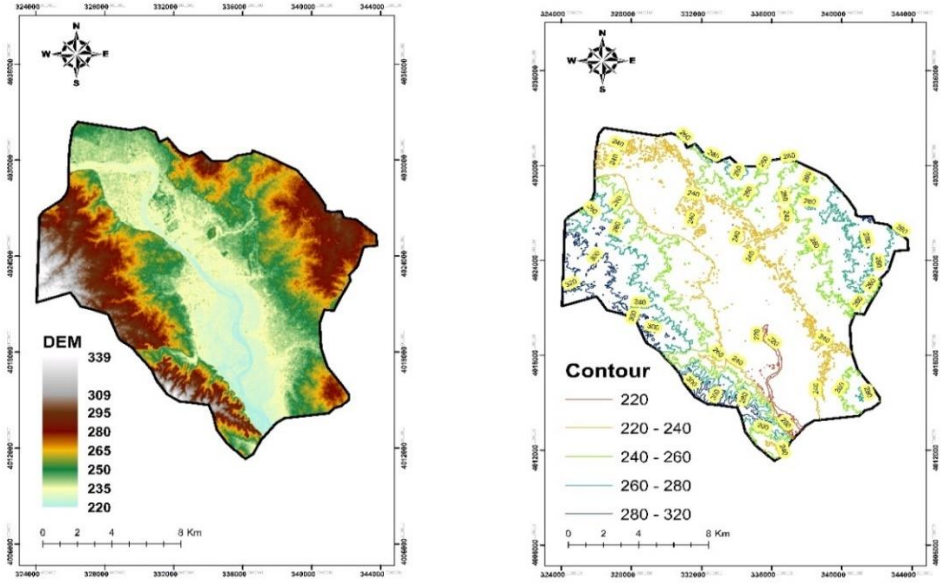

Figure 2: Natural characteristics of the study area DEM, Contour

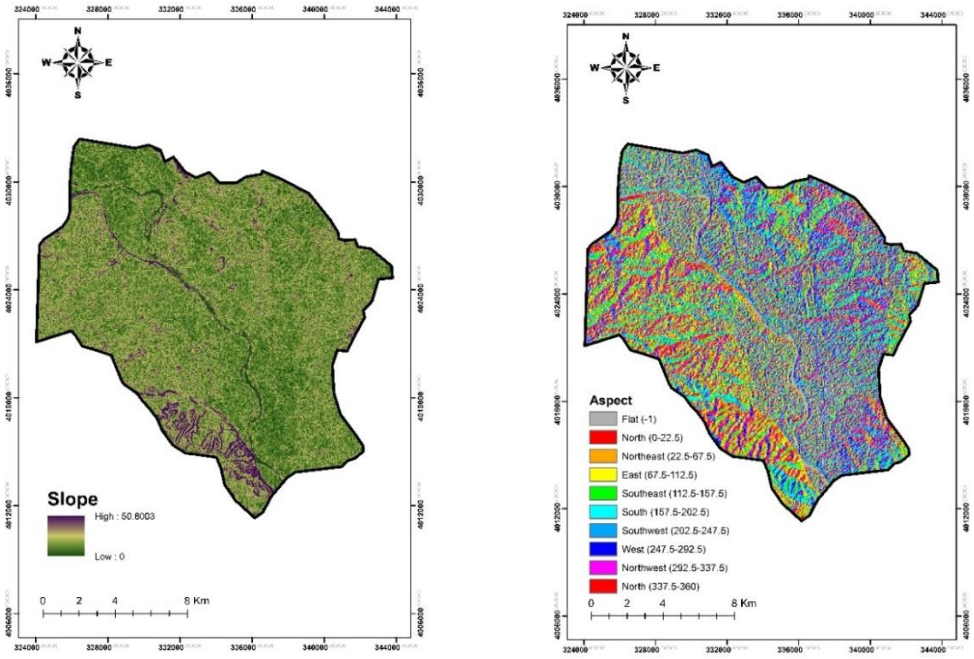

Figure 3 : Natural characteristics of the study area: Slope and Aspect.

3. Satellite data

The study used Landsat-8 images (collection_2 level_2) from the site http://earthexplorer.usgs.gov/; its resolution reaches 30 m. The NIR and RED wavelength spectra were used to study the characteristics of vegetation indicators, and the Thermal Infrared wavelength spectrum, which has a resolution of 100 m but is resampled to 30 m in delivered data product, to create maps measuring the Land surface temperature [21].

Table 1: The information about bands of landdsat8 collection2 level2 [22] and [21].

Name	Description	Resolution	Band Range (nm)
B01	Ultra Blue	30m	435-451
B02	Blue	30m	452-512
B03	Green	30m	533-590
B04	Red	30m	636-673
B05	Near Infrared (NIR)	30m	851-879
B06	Shortwave Infrared (SWIR) 1	30m	1566-1651
B07	Shortwave Infrared (SWIR) 2	30m	2107-2294
B10	Thermal Infrared (TIRS) 1	30m [1]	10600-11190

*[1]: TIRS bands were captured with a resolution of 100 m but resampled to 30 m in the given data output.

4. Methodology

The proportion of vegetation cover throughout the spring and summer seasons was assessed in 2015, 2018, and 2023. The NDVI was utilized. It was determined using band 5, which represents (NIR), and band 4 indicates (Red) [23], Table 3. To reduce the effect of the

soil background, the SAVI was calculated, where the spectral reflectance (Red) and (NIR) were used, as well as the addition of the adjustment factor (L) that helps to reduce the effect of the soil background and other environmental impact, which It makes it accurate in estimating plant activity in a variety of breeding conditions, with L values ranging from 0 to 1 as shown in Table 3 [24]. It not only calculates the Enhanced Vegetation Index2 (EVI2) but is also an upgraded version of the Enhanced Vegetation Index (EVI), which was created to eliminate atmospheric impacts. The equation is in Table 3. The Land Surface Temperature Index (LST) was also produced using Landsat8 Collection 2 Level-2 data from https://www.usgs.gov/ to determine how surface temperature affects vegetation. The NDBI, a spectral index used to detect urban areas, was derived using NIR and SWIR. The spectral range of NDBI is from 1 to -1, with positive values representing densely built-up areas and negative values representing unbuilt areas [25]. The NDWI index was relied upon to calculate water areas in Mosul, where two spectral bands were used: the green band and the near-infrared (NIR) band. The equation in Table 2 shows that the values are between -1 and 1. Positive values indicate water bodies [26].

Table 2 : NDVI values used in the selection of classes of vegetation [27].

Classes	NDVI
Water	< - 0.1
Bare soil	0.01 - 0.1
low vegetation	0.1 - 0.2
Sparse vegetation	0.2 - 0.4
Transition vegetation	0.4 - 0.6
Dense vegetation	> 0.6

Table 3: Spectral indices and their formula

No	Spectral Indices	Abbreviation	Formula	Reference
1	Normalized Difference Vegetation	NDVI	((NIR –RED) /(NIR + RED))	[28]
2	Adjusted Soil Vegetation Index	SAVI	((NIR-red) / (NIR+ red+ L). (1+L))	[29]
3	Enhanced Vegetation Index2	EVI2	(2.5×(NIR−RED) /(NIR+2.4×RED+1))	[30]
4	Land Surface Temperature	LST	((0.00341802 * DN + 149.0)-273.15)	[21]
5	Normalized Difference Built-up Index	NDBI	((SWIR - NIR) / (SWIR + NIR))	[25]
6	Normalized Difference Water Index	NDWI	((Green - NIR) / (Green - NIR))	[26]

To study spectral vegetation indicators, it is critical to understand their interaction with land surface temperature. Therefore, all statistical analyses were performed in Excel 2013. Descriptive statistics were produced for all data sets used in this study to help understand the preliminary data summary. The Pearson correlation test assessed the linear association between land surface temperature and vegetation index. In addition, a simple linear regression was performed between LST and other spectral indicators to describe the behavior of the studied indicators.

5. Results and Discussion

The NDVI index values were extracted from the equation in Table 3, and the change was evident in the size, spread, density, and distribution of vegetation cover between 2015, 2018, and 2023 for the spring and summer seasons. The NDVI values in 2015 for the spring season indicated an apparent increase in values, as the range was -0.164309 to 0.536274, while in the summer, the range was -0.0329901 to 0.435515, and in 2018, the spring month, the range was -0.148987 to 0.534253, and the range for the summer was -0.182405 to 0.528132, but in 2023

the range for the spring was -0.0815459 to 0.4 79428 and range for summer was -0.115044 to 0.478071, Figure 4.

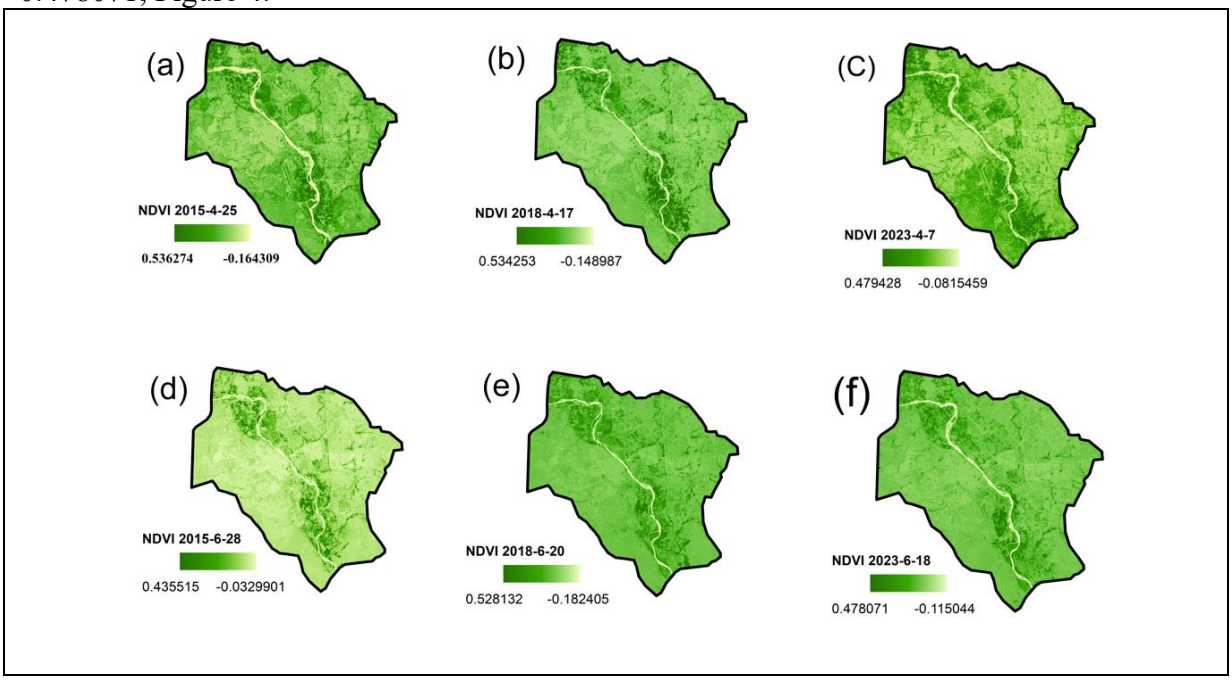

Figure 4: NDVI maps for the (a) 2015-4-25, (b) 2018-4-17, (c) 2023-4-7, (d) 2015-6-28, (e) 2018-6-20, (f) 2023-6-18

The results of the SAVI index showed values that were relatively close to the lower values of the EVI2 index, where the SAVI values in 2015, the spring season, were in the range of -0.246457 to 0.8044, while the range for the summer season was -0.0494841 to 0.653264, and in 2018, the spring season was -0.223476 to 0.801369. The range for the summer is -0.2736 to 0.792188, and in 2023, the range for the spring is -0.122316 to 0.719132, and the range for the summer is -0.172562 to 0.717097. Therefore, the SAVI index is a hybrid of the NDVI index depending on the soil parameter. Figure 4 shows the SAVI maps.

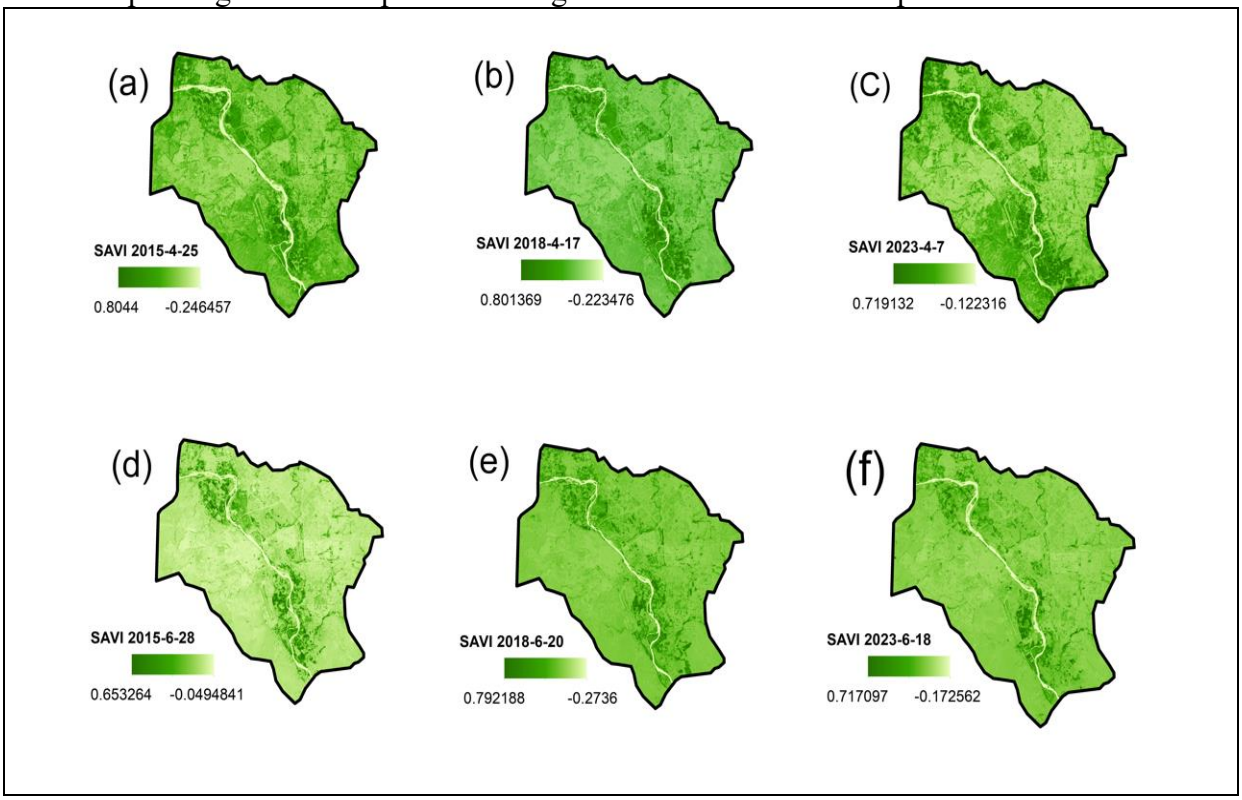

Figure 5: SAVI maps for the (a) 2015-4-25, (b) 2018-4-17, (c) 2023-4-7, (d) 2015-6-28, (e) 2018-6-20, (f) 2023-6-18

Enhanced vegetation index2 (EVI2), which was developed and modified by [31] to eliminate the effect of the atmosphere and terrain in calculating vegetation values, was modified from the Enhanced vegetation index (EVI). Accordingly, this index was tested on the study area, and values for vegetation cover were extracted in Figure 5, where maps were revealed. The index reflects the density of vegetation in irrigated agricultural areas. In 2015, the spring season was -0.226313 to 1.01212, the summer range was -0.0478635 to 0.7804, and in 2018, the spring season, the range was -0.206429 to 1.00723, the summer range -0.249496 to 0.992481, while in 2023 the spring range was -0.116021 to 0.878441 and the summer range was -0.161526 to 0.875346

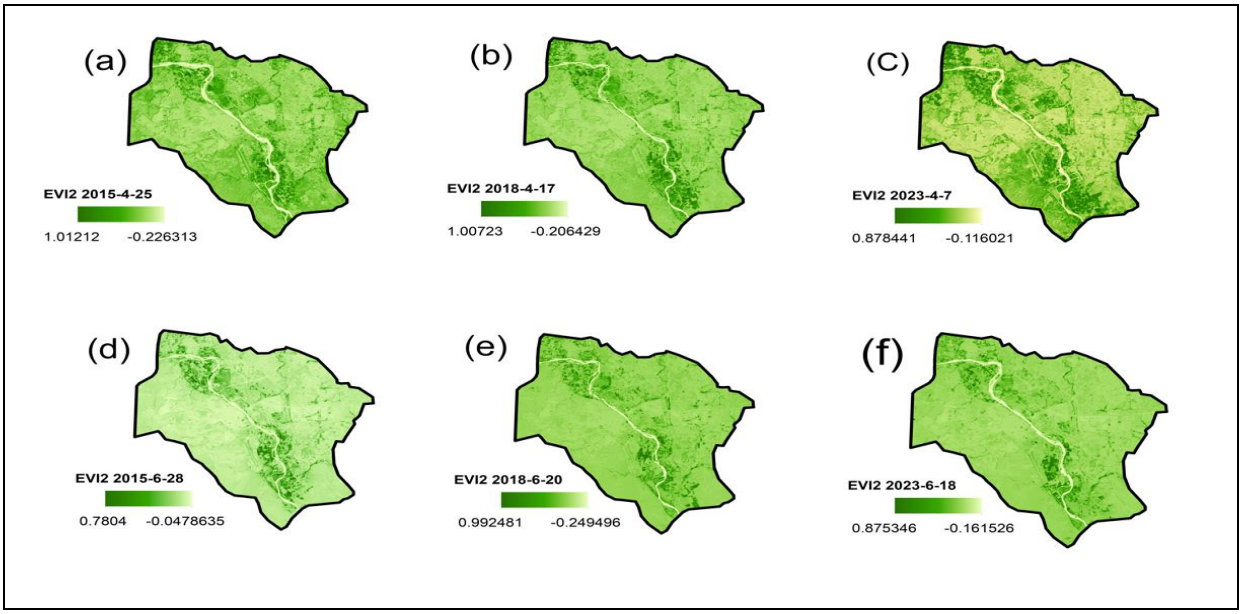

Figure 6: EVI2 maps for the (a) 2015-4-25, (b) 2018-4-17, (c) 2023-4-7, (d) 2015-6-28, (e) 2018-6-20, (f) 2023-6-18

For all three indicators used, vegetation cover values were extracted, as is clear in the previous maps. Table 3 shows the percentages of vegetation cover for each year and notes the changes that occurred and what caused these changes, as the lowest percentage of vegetation cover was in 2015 when it reached 13% in the Spring season, and the percentage of vegetation cover decreased to 4% due to the rise in temperature that year for the NDVI and SAVI indicators. As for the EVI2 indicator, noticing an increase in the percentages to 16% in spring and 5% in summer. This indicates that the best index for measuring vegetation cover is EVI2, which gives accurate values far from the effects of the Atmosphere: In 2018, the percentage of vegetation cover decreased to 10% in summer due to the exposure of the Mosul forests to a fire in 2017, but the difference between spring and summer was less than in 2015, when it reached 6% in summer, due to the decrease in temperature for the two indices, NDVI. SAVI, EVI2 is 11.30% in the spring and 6.90% in the summer. In 2023, the vegetation cover increased in certain areas, as the percentage became 19% in the spring according to two indices, NDVI and SAVI, where the appearance of permanent plants was observed due to their loss in the summer, where the percentage decreased to 5% due to the rise in temperature

and the impact of forest fires in 2022 with a high percentage and in 2021 with a high percentage. Low as for the EVI2 index, 21.70% in the spring and 5.30% in the summer.

Table 4: The Percentages of vegetation indicators

Study years	NDVI	SAVI	EVI2
4/25/2015	13%	13%	16%
6/28/2015	4%	4%	5%
4/17/2018	10%	10%	11.30%
6/20/2018	6%	6%	6.90%
4/7/2023	19%	19%	21.70%
6/18/2023	5%	5%	5.30%

The results of Land surface temperature showed a significant effect on vegetation density, Figure 6, between the spring and summer seasons in 2015 April, the LST range of 16.1563 to 45.4112, while in 2015 June, the spectral range 24.739 to 65.7176. In April 2018, the LST range was 20.1691 to 38.6708, while in June 2018, the range was 28.4475 to 61.469. In April 2023, the spectral range was 17.8346 to 38.5648; in June 2023, the range was 26.9743 to 57.8664.

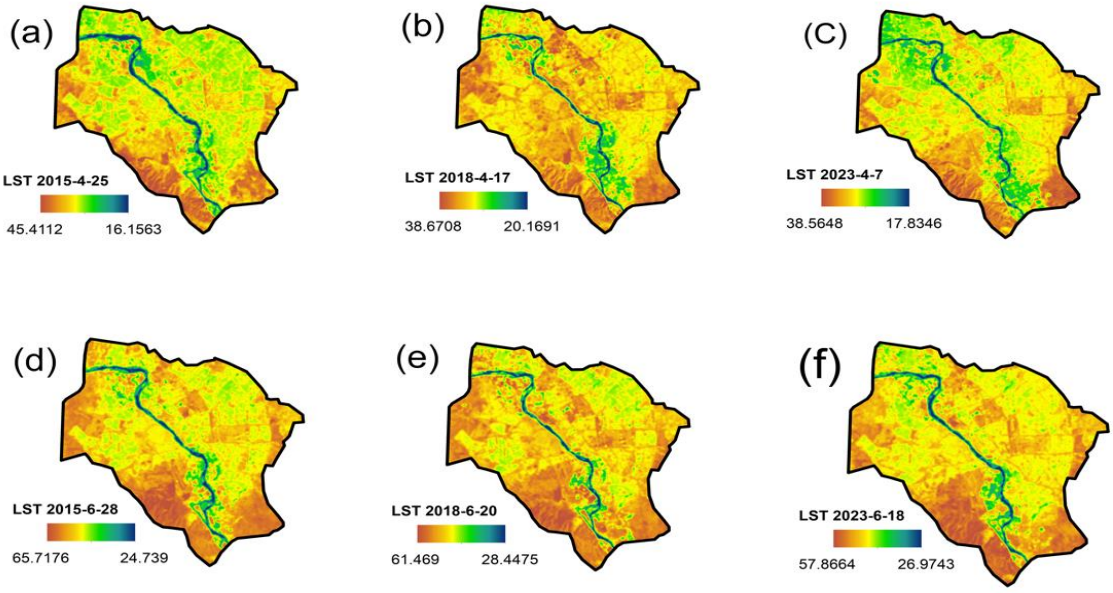

Figure 7: LST maps for the (a) 2015-4-25, (b) 2018-4-17, (c) 2023-4-7, (d) 2015-6-28, (e) 2018-6-20, (f) 2023-6-18.

The percentage of urban areas reached approximately 35% in 2015, and the percentage increased in 2018, reaching 39%, until it reached 42% in 2023. Table 4 shows the difference in urban development over the three years. Figure 8 shows maps of urban areas.

Table 5: Percentages of building indicator

Index	4/25/2015	4/17/2018	4/7/2023	6/28/2015	6/20/2018	6/18/2023
NDBI	35%	39%	42%	34%	39%	42%

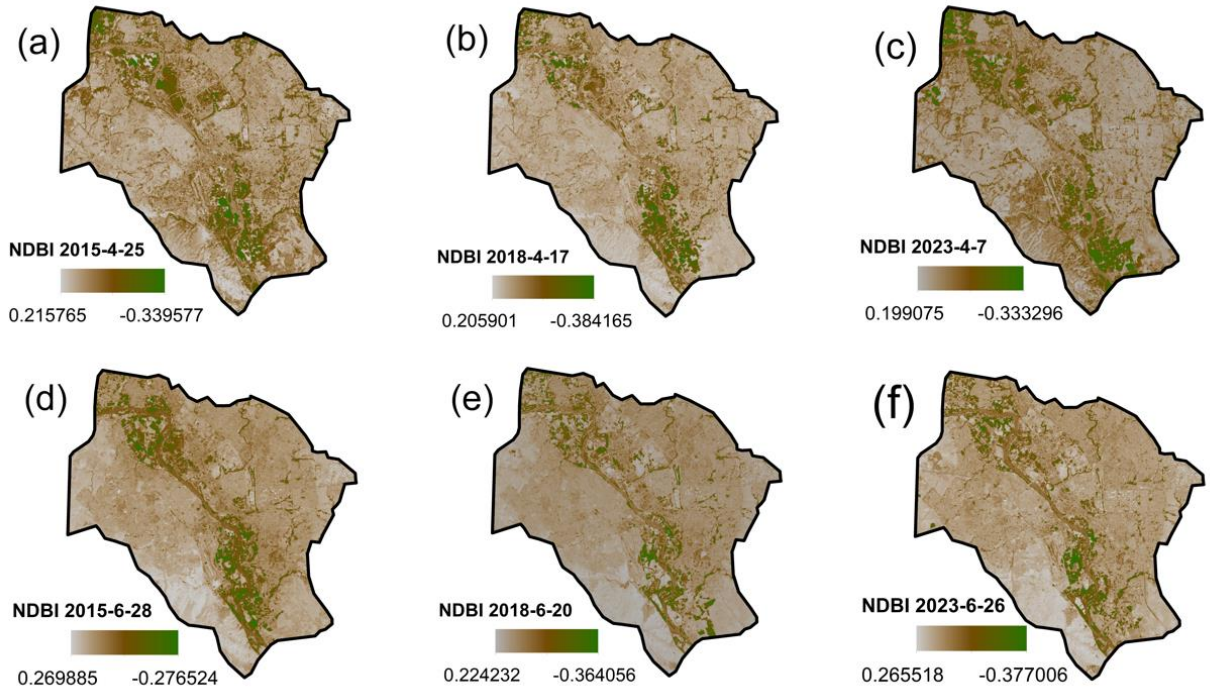

Figure 8: NDBI maps for the (a) 2015-4-25, (b) 2018-4-17, (c) 2023-4-7, (d) 2015-6-28, (e) 2018-6-20, (f) 2023-6-18.

As for water bodies, it was 2.80% in 2015 and decreased in 2018 to 1.80%, and in 2023, the percentage increased to 2.10%, as shown in Table 5. Figure 9 shows maps of water bodies.

Table 6: Percentages of water indicator

Index	4/25/2015	4/17/2018	4/7/2023	6/28/2015	6/20/2018	6/18/2023
NDWI	2.80%	1.80%	2.10%	2.10%	1.80%	2.10%

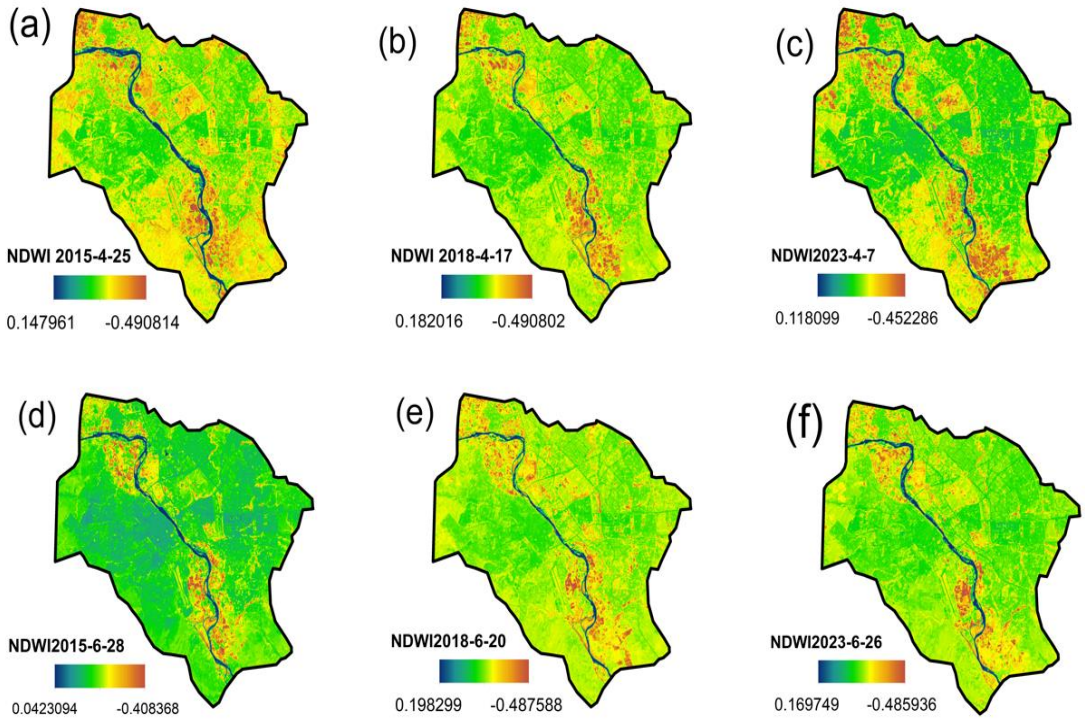

Figure 9:NDWI maps for the (a) 2015-4-25, (b) 2018-4-17, (c) 2023-4-7, (d) 2015-6-28, (e) 2018-6-20, (f) 2023-6-18.

In order to evaluate the change in vegetation cover, it is necessary to know the correlation between vegetation indicators and the Earth's surface temperature index, as it was found that there is a strong inverse relationship with statistical significance that there is a strong effect of temperature on the vegetation cover of the study area. Correlation and regression results for NDVI in April 2015 (r=0.066156, R^2 = 0.0026) and in June 2015 (r= -0.25083, R^2 = 0.0002). April 2018 (r= -0.19299, R^2 = 0.0004) and June 2018 (r= -0.06818, R^2 = 0.0709). In April 2023 (r= -0.07452, R^2 = 0.0149) and June 2023 (r= -0.05301, R^2 = 0.0952), Table 7.

Table 7: A Pearson correlation simple linear regression between LST&NDVI

Years	LST&NDVI
4/25/2015	y = -9E-06x + 0.1269 r=0.066156 R^2 = 0.0026
6/28/2015	y = -2E-06x + 0.0869 r= -0.25083 R^2 = 0.0002
4/17/2018	y = -4E-06x + 0.1078 r= -0.19299 R^2 = 0.0004
6/20/2018	y = -0.0027x + 52.764 r= -0.06818 R^2 = 0.0709
4/7/2023	y = -2E-05x + 0.1512 r= -0.07452 R^2 = 0.0149
6/26/2023	y = -0.0021x + 52.624 r=-0.01965 R^2 = 0.0342
6/18/2023	y = -0.0031x + 49.691 r= -0.05301 R^2 = 0.0952

a)25 April 2015 b)28 June 2015

y = -9E-06x + 0.1269 ,r=0.066156, R^2 = 0.0026 y = -2E-06x + 0.0869 , r= -0.25083 , R^2 = 0.0002

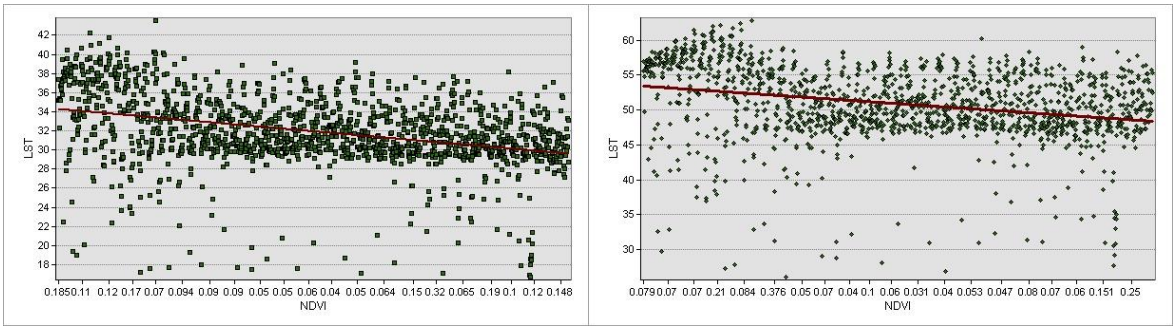

c)17 April 2018 d) 20 June 2018

y = -4E-06x + 0.1078 , r= -0.19299 , R^2 = 0.0004

y = -0.0027x + 52.764 , r= -0.06818, R^2 = 0.0709

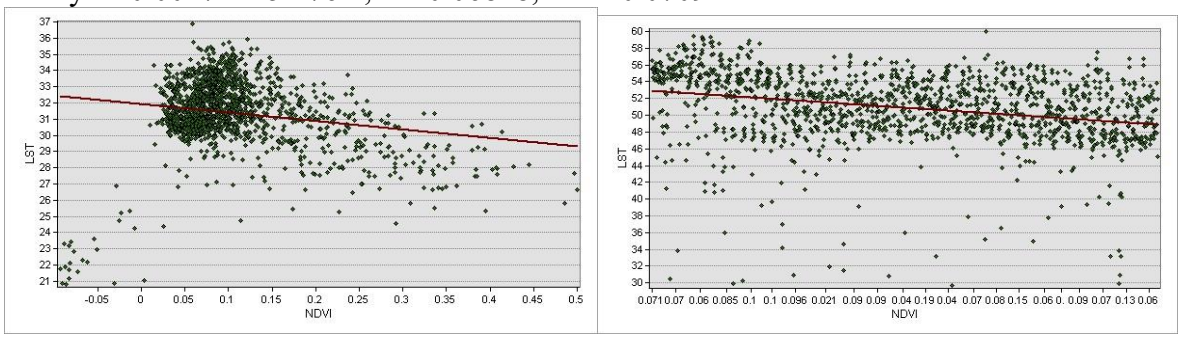

e)7 April 2023 f) 18 June 2023

y = -2E-05x + 0.1512 , r= -0.07452 ,R^2 = 0.0149

y = -0.0031x + 49.691 r= -0.05301 R^2 = 0.0952

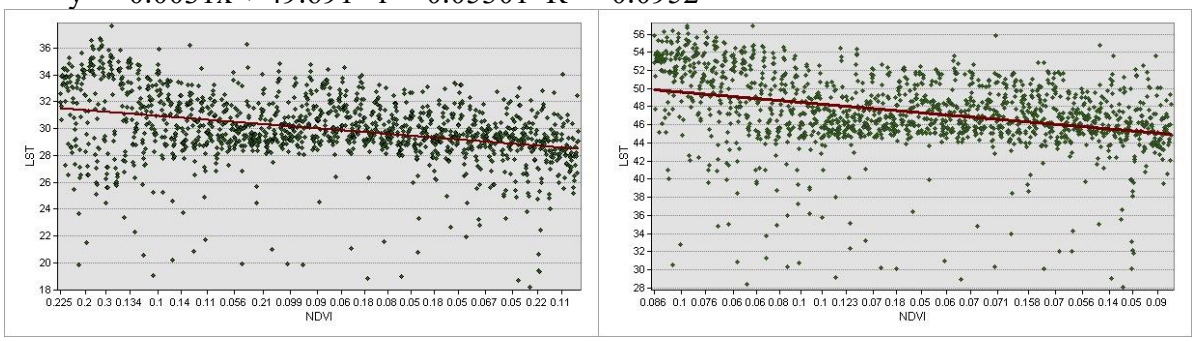

Figure 10: Results of Pearson correlation and Simple linear regression between NDVI and LST, (a) 2015-4-25, (b) 2018-4-17, (c) 2023-4-7, (d) 2015-6-28, (e) 2018-6-20, (f) 2023-6-18.

Results of Pearson correlation and simple linear regression between SAVI and LST in April 2015 (r= 0.066157, R^2 = 0.0026) and in 2015 (June (r= -0.25083, R^2 = 0.0003). April 2018 (r= - 0.19299, R^2 = 0.0004) and June 2018 (r= -0.06819, R^2 = 0.0001). In April 2023 (r= -0.07452, R^2 = 0.1059) and in June 2023 (r= -0.05301, R^2 = 0.0952), Table 8 and (Figure 11).

Table 8: A Pearson correlation simple linear regression between LST&SAVI

Years	LST&SAVI
4/25/2015	y = -1E-05x + 0.1904 r= 0.066157 R^2 = 0.0026
6/28/2015	y = -3E-06x + 0.1308 r= -0.25083 R^2 = 0.0003
4/17/2018	y = -5E-06x + 0.1617 r= -0.19299 R^2 = 0.0004
6/20/2018	y = 2E-06x + 0.1225 r= -0.06819 R^2 = 0.0001
4/7/2023	y = -0.002x + 31.377 r= -0.07452 R^2 = 0.1059
6/26/2023	y = -7E-06x + 0.1284 r= -0.01965 R^2 = 0.0011
6/18/2023	y = -0.0031x + 49.691 r= -0.05301 R^2 = 0.0952

a)25 April 2015 b)28 June 2015

y = -1E-05x + 0.1904, r= 0.06615, R^2 = 0.0026

y = -3E-06x + 0.1308, r= -0.25083,R^2 = 0.0003

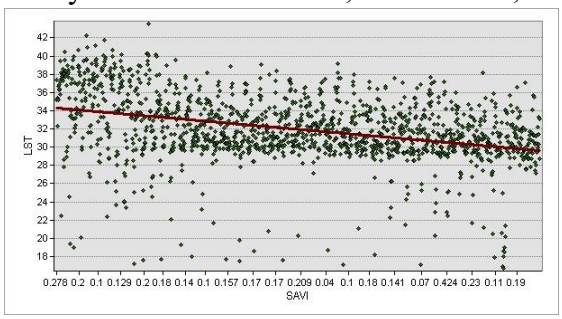

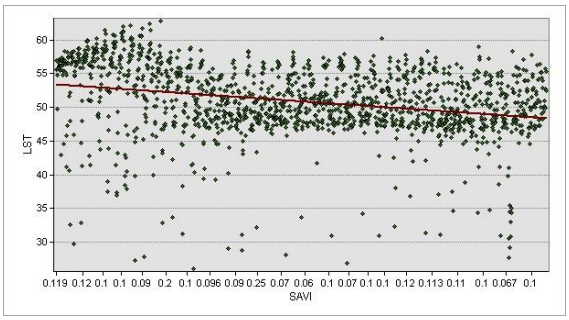

c)17 April 2018 d)20 June 2018

y = -5E-06x + 0.1617, r= -0.19299, R^2 = 0.0004

y = 2E-06x + 0.1225 ,r= -0.06819, R^2 = 0.0001

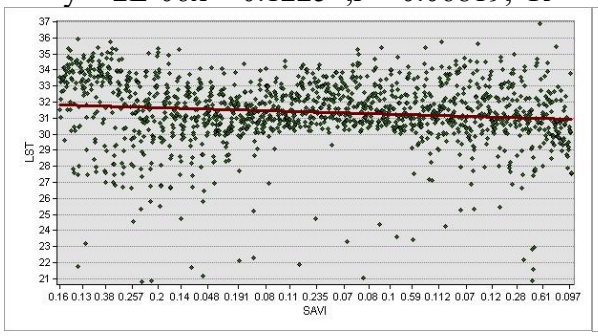

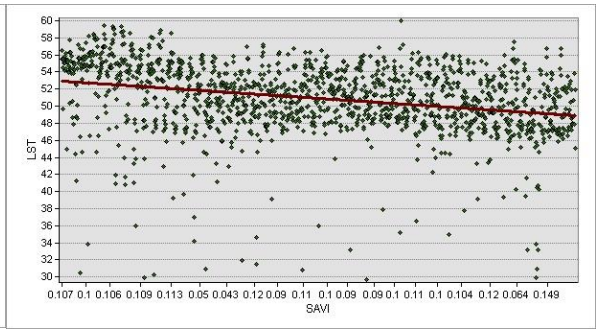

e)7 April 2023 f)18 June 2023

y = -0.002x + 31.377, r= -0.0745, R^2 = 0.1059

y = -0.0031x + 49.691 r= -0.05301 R^2 = 0.0952

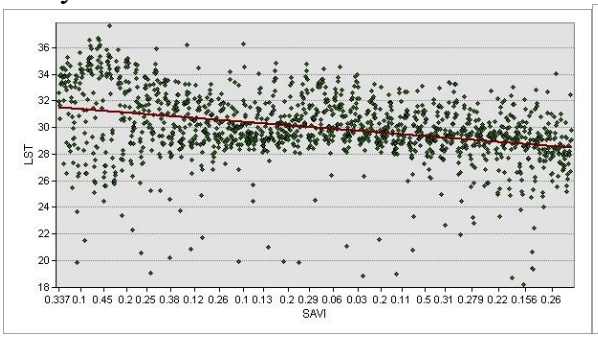

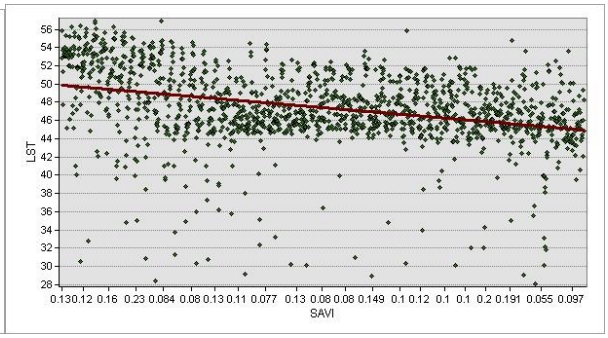

Figure 11: Results of Pearson correlation and Simple linear regression between SAVI and LST, (a) 2015-4-25, (b) 2018-4-17, (c) 2023-4-7, (d) 2015-6-28, (e) 2018-6-20, (f) 2023-6-18.

Results of Pearson correlation and simple linear regression between EVI2 and LST in April 2015 (r= 0.03715 R^2 = 0.0026) and June 2015 (r= -0.25956, R^2 = 0.0003). In April 2018

(r= -0.25956, R^2 = 0.0003) June 2018 (r=-0.09444, R^2 = 8E-05). In April 2023 (r= -0.10222, R^2 = 0.0135) and in June 2023 (r=- 0.07984 R^2 = 0.095), Table 9 and (Figure 12).

Table 9: A Pearson correlation and simple linear regression between LST&EVI2.

Years	LST&EVI2
4/25/2015	y = -1E-05x + 0.1904 r= 0.03715 R^2 = 0.0026
6/28/2015	y = -3E-06x + 0.1344 r= -0.25956 R^2 = 0.0003
4/17/2018	y = -6E-06x + 0.1704 r= -0.2198 R^2 = 0.0004
6/20/2018	y = 2E-06x + 0.127 r= -0.09444 R^2 = 8E-05
4/7/2023	y = -4E-05x + 0.2424 r= -0.10222 R^2 = 0.0135
6/26/2023	y = -8E-06x + 0.1337 r= -0.05237 R^2 = 0.0011
6/18/2023	y = -0.0031x + 49.691 r=- 0.07984 R^2 = 0.0952

a)25 April 2015 b)28 June 2015

y = -1E-05x + 0.1904 ,r= 0.03715 , R^2 = 0.0026 y = -3E-06x + 0.1344, r= -0.25956, R^2 = 0.0003

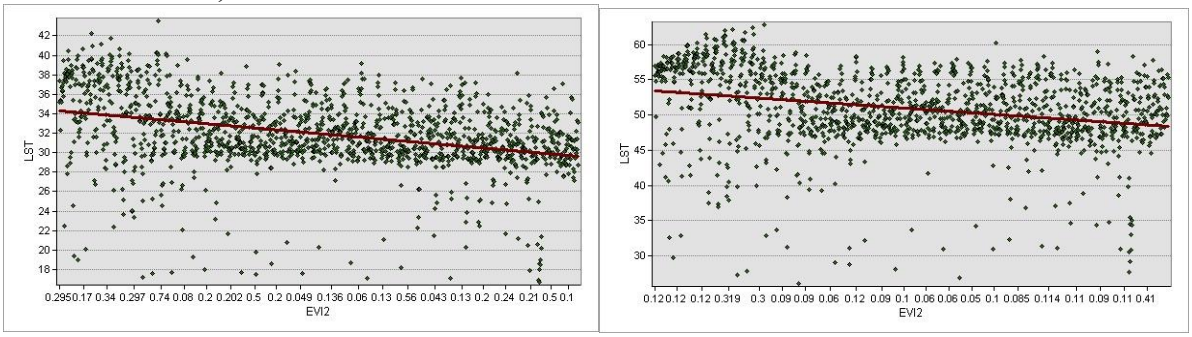

c)17 April 2018 d)20 June 2018

y = -6E-06x + 0.1704 , r= -0.2198 , R^2 = 0.0004 y = 2 r= -0.09444 , R^2 = 8E-05

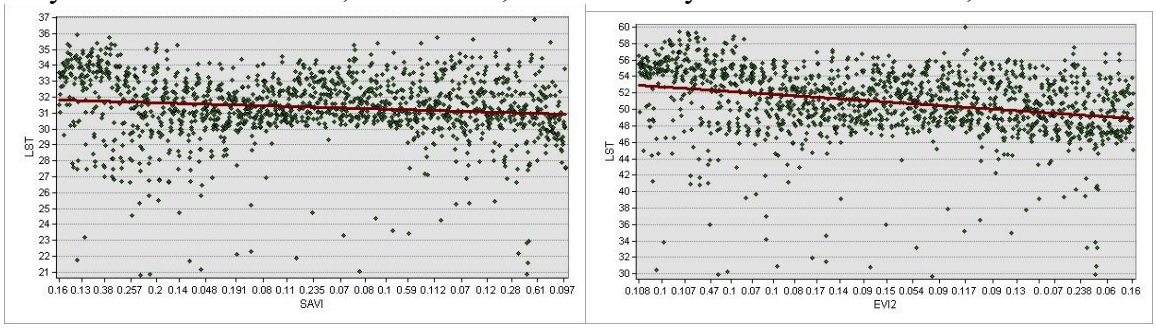

e)7 April 2023 f) 18 June 2023

y = -4E-05x + 0.2424 , r= -0.10222, R^2 = 0.0135 y = -0.0031x + 49.691 r=- 0.07984 R^2 = 0.0952

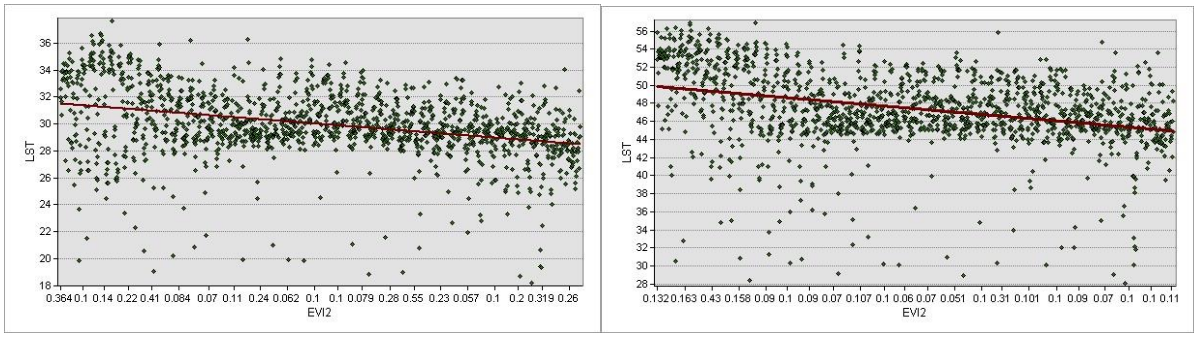

Figure 12: Results of Pearson correlation and Simple linear regression between EVI2 and LST, (a) 2015-4-25, (b) 2018-4-17, (c) 2023-4-7, (d) 2015-6-28, (e) 2018-6-20, (f) 2023-6-18.

The most important indicator through which temperature is calculated and the extent to which fires are affected is the LST index, where the difference in the spatial distribution of temperature was observed due to the occurrence of fires in different areas [32]. Many studies have confirmed the occurrence of fires and the loss of a percentage of vegetation cover, which leads to an increase in LST values [33].

. 1-Conclusions

The temperature rise has a significant impact on the vegetation cover of Mosul city and is the main factor in the lack of vegetation cover, which helps in the occurrence of fires. Fires occurred in Mosul forests for three years: the first (12-05-2017), the second (06-07-2021), and the third (6-29-2022). A strong inverse relationship was obtained between LST and the vegetation cover indices NDVI, SAVI, and EVI2. This study revealed that the highest percentage of vegetation cover in 2015, the fourth month, was due to low temperatures and lack of exposure to fires, and the lowest percentage was in 2015, the sixth month. This indicates the lack of drama in the vegetation cover and the rise in temperatures more than in 2018 and 2023 in both years. Noticing that afforestation operations are taking place in several areas, noticing the presence of barren lands in the areas exposed to fires, it is necessary to afforestation the areas to restore them to what they were. Afforestation also leads to reducing high temperatures and removing harmful weeds because they are a strong factor in the spread of fires.

References

[1] H. Mohammad, H. Al-Bilbisi, and H. A. Sammour, "Detect and analyze change in vegetation cover using spectral vegetation indicators," *Dirasat: Human and Social Sciences,* vol. 45, no. 1, 2018.

[2] S. C. Moser, "A partial instructional module on global and regional land use/cover change: assessing the data and searching for general relationships," *GeoJournal,* vol. 39, pp. 241-283, 1996.

[3] A. Ansari and M. H. Golabi, "Prediction of spatial land use changes based on LCM in a GIS environment for Desert Wetlands–A case study: Meighan Wetland, Iran," *International soil and water conservation research,* vol. 7, no. 1, pp. 64-70, 2019.

[4] T. S. Hashesh and B. A. Ahmed, "Using GIS and remote sensing to study water quality changes and spectral analysis for Al-hawizah marshes, South of Iraq," *Iraqi Journal of Science,* pp. 1757-1768, 2018.

[5] D. Alexakis *et al.*, "GIS and remote sensing techniques for the assessment of land use change impact on flood hydrology: the case study of Yialias basin in Cyprus," *Natural Hazards and Earth System Sciences,* vol. 14, no. 2, pp. 413-426, 2014.

[6] E. Yirsaw, W. Wu, X. Shi, H. Temesgen, and B. Bekele, "Land use/land cover change modeling and the prediction of subsequent changes in ecosystem service values in a coastal area of China, the Su-Xi-Chang Region," *Sustainability,* vol. 9, no. 7, p. 1204, 2017.

[7] S. K. Patel, P. Verma, and G. Shankar Singh, "Agricultural growth and land use land cover change in peri-urban India," *Environmental monitoring and assessment,* vol. 191, pp. 1-17, 2019.

[8] K. Islam, M. Jasimuddin, B. Nath, and T. K. Nath, "Quantitative Assessment of land cover change using Landsat time series data: case of Chunati Wildlife Sanctuary (CWS), Bangladesh," *International Journal of Environment and Geoinformatics,* vol. 3, no. 2, pp. 45-55, 2016.

[9] B. Liu, J. Chen, J. Chen, and W. Zhang, "Land cover change detection using multiple shape parameters of spectral and NDVI curves," *Remote Sensing,* vol. 10, no. 8, p. 1251, 2018.

[10] R. A. Dawson, G. P. Petropoulos, L. Toulios, and P. K. Srivastava, "Mapping and monitoring of the land use/cover changes in the wider area of Itanos, Crete, using very high resolution EO imagery with specific interest in archaeological sites," *Environment, development and sustainability,* vol. 22, no. 4, pp. 3433-3460, 2020.

[11] M. C. Anderson, R. G. Allen, A. Morse, and W. P. Kustas, "Use of Landsat thermal imagery in monitoring evapotranspiration and managing water resources," *Remote sensing of environment,* vol. 122, pp. 50-65, 2012.
[12] J. B. Fisher *et al.*, "The future of evapotranspiration: Global requirements for ecosystem functioning, carbon and climate feedbacks, agricultural management, and water resources," *Water resources research,* vol. 53, no. 4, pp. 2618-2626, 2017.
[13] H. Su, M. F. McCabe, E. F. Wood, Z. Su, and J. Prueger, "Modeling evapotranspiration during SMACEX: Comparing two approaches for local-and regional-scale prediction," *Journal of hydrometeorology,* vol. 6, no. 6, pp. 910-922, 2005.
[14] W. Kustas, J. Alfieri, H. Nieto, T. Wilson, F. Gao, and M. Anderson, "Utility of the two-source energy balance (TSEB) model in vine and interrow flux partitioning over the growing season," *Irrigation Science,* vol. 37, pp. 375-388, 2019.
[15] M. Allawai and B. Ahmed, "Using remote sensing and GIS in measuring vegetation cover change from satellite imagery in Mosul City, North of Iraq," in *IOP conference series: materials science and engineering*, 2020, vol. 757, no. 1: IOP Publishing, p. 012062.
[16] M. M. Rahman, "Temporal change detection of vegetation coverage in Patuakhali Coastal Area of Bangladesh using GIS & remotely sensed data," *International Journal of Geomatics and Geosciences,* vol. 4, no. 1, pp. 36-46, 2013.
[17] M. S. Hossain *et al.*, "Spatiotemporal change detection of land use land cover (LULC) in Fashiakhali wildlife sanctuary (FKWS) impact area, Bangladesh, employing multispectral images and GIS," *Modeling Earth Systems and Environment,* vol. 9, no. 3, pp. 3151-3173, 2023.
[18] A. Sekertekin and S. Bonafoni, "Sensitivity analysis and validation of daytime and nighttime land surface temperature retrievals from Landsat 8 using different algorithms and emissivity models," *Remote Sensing,* vol. 12, no. 17, p. 2776, 2020.
[19] A. S. Shihab, "Assessment of ambient air quality of Mosul city/Iraq via Air Quality Index," *Journal of Ecological Engineering,* vol. 22, no. 10, 2021.
[20] A. A. Al-Shammari and M. A. Al-Dabbas, "Extraction Drainage Network for Lesser Zab River Basin from DEM using Model Builder in GIS," *Iraqi Journal of Science,* vol. 56, no. 4A, pp. 2915-2926, 2015.
[21] U. Landsat, "Landsat 8-9 Operational Land Imager (OLI)—Thermal Infrared Sensor (TIRS) Collection 2 Level 2 (L2) Data Format Control Book (DFCB)," *United States Geological Survey: Reston, VA, USA,* vol. 78, 2020.
[22] https://docs.sentinel-hub.com/api/latest/data/landsat-8-l2/, "About Landsat 8-9 OLI-TIRS Collection 2 Level 2 Data," 2022.
[23] S. Huang, L. Tang, J. P. Hupy, Y. Wang, and G. Shao, "A commentary review on the use of normalized difference vegetation index (NDVI) in the era of popular remote sensing," *Journal of Forestry Research,* vol. 32, no. 1, pp. 1-6, 2021.
[24] Z. Zhen *et al.*, "Using the negative soil adjustment factor of soil adjusted vegetation index (SAVI) to resist saturation effects and estimate leaf area index (LAI) in dense vegetation areas," *Sensors,* vol. 21, no. 6, p. 2115, 2021.
[25] O. A. R. Yousef and H. S. Jaber, "Studying the Environmental Changes Using Remote Sensing and GIS," *Iraqi Journal of Science,* pp. 3705-3716, 2023.
[26] N. Waleed and A. B. Maythm, "Monitoring the Expansion of Unplanned Urbanization and its Impact on Climate Change based on Google Earth Engine Service, a Case Study of Baghdad/Iraq," *Iraqi Journal of Science,* pp. 1160-1171, 2024.
[27] L. M. de Aquino França, J. A. dos Santos Pereira, and J. D. Galvíncio, "CLIMATE CHARACTERIZATION USING WATER BALANCE AND NDVI FOR CITY OF PAULISTA-PE," *Journal of Hyperspectral Remote Sensing,* vol. 2, no. 2, pp. 025-036, 2012.
[28] M. Ahmed and W. Ahmad, "Using normalized difference vegetation index (NDVI) to assessment the changes of vegetations cover In surrounding area of Himreen Lake," *Iraqi Journal of Science,* vol. 54, no. 4, pp. 895-901, 2013.
[29] A. A. Salman and F. K. M. Al Ramahi, "Detection of Spectral Reflective Changes for Temporal Resolution of Land Cover (LC) for Two Different Seasons in Central Iraq," *Iraqi Journal of Science,* pp. 5589-5603, 2022.

[30] P. Mondal, "Quantifying surface gradients with a 2-band Enhanced Vegetation Index (EVI2)," *Ecological Indicators,* vol. 11, no. 3, pp. 918-924, 2011.

[31] Z. Jiang, A. R. Huete, K. Didan, and T. Miura, "Development of a two-band enhanced vegetation index without a blue band," *Remote sensing of Environment,* vol. 112, no. 10, pp. 3833-3845, 2008.

[32] M. Montes-Helu *et al.*, "Persistent effects of fire-induced vegetation change on energy partitioning and evapotranspiration in ponderosa pine forests," *Agricultural and forest meteorology,* vol. 149, no. 3-4, pp. 491-500, 2009.

[33] E. Lambin, K. Goyvaerts, and C. Petit, "Remotely-sensed indicators of burning efficiency of savannah and forest fires," *International Journal of Remote Sensing,* vol. 24, no. 15, pp. 3105-3118, 2003.